Journal of
Synchrotron
Radiation

ISSN 0909-0495

Received 11 December 2007
Accepted 7 March 2008

X-ray photon correlation spectroscopy under flow

Andrei Fluerasu,[a]* Abdellatif Moussaïd,[a] Péter Falus,[b] Henri Gleyzolle[a] and Anders Madsen[a]

[a]Troïka (ID10A) Beamline, European Synchrotron Radiation Facility, Grenoble, France, and [b]Institut Laue Langevin, Grenoble, France. E-mail: fluerasu@esrf.fr

X-ray photon correlation spectroscopy was used to probe the diffusive dynamics of colloidal particles in a shear flow. Combining X-ray techniques with microfluidics is an experimental strategy that reduces the risk of X-ray-induced beam damage and also allows time-resolved studies of processes taking place in flow cells. The experimental results and theoretical predictions presented here show that in the low shear limit for a 'transverse flow' scattering geometry (scattering wavevector **q** perpendicular to the direction of flow) the measured relaxation times are independent of the flow rate and determined only by the diffusive motion of the particles. This is not generally valid and, in particular, for a 'longitudinal flow' (**q** ∥ flow) scattering geometry the relaxation times are strongly affected by the flow-induced motion of the particles. The results here show that the Brownian diffusion of colloidal particles can be measured in a flowing sample and that, up to flux limitations, the experimental conditions under which this is possible are easier to achieve at higher values of q.

Keywords: coherent X-ray diffraction; X-ray photon correlation spectroscopy; dynamics; colloids; flow; microfluidics.

1. Introduction

Over the past decade, X-ray photon correlation spectroscopy (XPCS) has emerged as a unique experimental tool that allows the direct measurement of fluctuations in a large number of condensed matter systems (Sutton, 2002). It provides a method complementary to dynamic light scattering (DLS) (Berne & Pecora, 2000) for the observation of mesoscale dynamics (*e.g.* 1 nm–1 μm length scales) in opaque materials or in samples where multiple scattering limits the applicability of DLS. Indeed, a problem more commonly encountered with X-rays is a small scattering cross section, which means that multiple scattering can usually be neglected, but also that very intense beams are required to achieve reasonable signal-to-noise ratios. As a consequence, XPCS experiments have become possible only at high-brilliance synchrotron radiation sources.

In many recent applications, XPCS has been used to study bulk equilibrium and/or non-equilibrium mesoscale dynamics in a large class of complex fluids including, but not being limited to, colloidal suspensions (Banchio *et al.*, 2006), colloidal gels (Fluerasu *et al.*, 2007) or polymer-based systems (Falus *et al.*, 2006). However, irradiation damage is often encountered when intense X-ray beams are employed to study soft-matter or biological samples. This problem will become even more important at the next generation of light sources, X-ray free-electron lasers and energy-recovery linacs, with their unprecedented brilliance, stronger by several orders of magnitude than present third-generation synchrotron radiation sources (Shenoy, 2003; Bilderback *et al.*, 2005). Flowing a fluid sample through a microfluidic device while performing XPCS provides a method that can limit the beam-induced damage effects and may allow the direct measurement of slow mesoscale dynamics in various 'X-ray sensitive' systems (*e.g.* colloids, polymers and bio-polymers, gels, aggregating proteins *etc.*). In addition, this experimental strategy offers the possibility to perform time-resolved experiments. If a process like protein folding (Pollack *et al.*, 2001) occurs in a microfluidic device, the time-dependence of the kinetics is mapped into a spatial-dependence of stationary properties along the microfluidic channel. In such an experimental configuration, XPCS could be used to study the time-dependence of dynamical properties even for very weakly scattering systems (*e.g.* formation of colloid and polymer gels, aggregating proteins).

In the experiments reported here, the dynamics of a colloidal suspension of hard spheres in a shear flow were studied by XPCS. These results provide, to our knowledge, the first feasibility study of XPCS as a probe for the diffusive dynamics in a flowing sample. In the visible range, similar experiments have been performed by Ackerson & Clark (1981) using DLS. Here we show that, with the higher values of the scattering wavevector **q** probed by X-rays, it is easier to achieve the experimental conditions under which the diffusive dynamics are accessible.

XPCS employs a partially coherent X-ray beam which creates, when scattered from a disordered sample, a char-

acteristic speckle pattern reflecting the instantaneous spatial arrangement of the scatterers (Sutton *et al.*, 1991). The technique consists of monitoring the temporal correlations of the speckle fluctuations, which are caused by the motion of the scatterers in the sample.

With a dilute colloidal suspension under shear flow, the correlation functions measured by XPCS are not only determined by the random (Brownian) motion of the colloids but are also affected by their flow-induced motion. As shown in the following, the correlation functions are strongly influenced by the Doppler shifts resulting from particles moving at different average flow velocities owing to the shear. The intensity scattered by particles moving with an average velocity difference of $\delta\mathbf{v}$ creates a signal on the detector that is modulated by a self-beat frequency of $\mathbf{q}\cdot\delta\mathbf{v}$ (Fuller *et al.*, 1980). Hence a homodyne photon correlation spectroscopy experiment can measure velocity gradients but not the absolute velocity, which is only accessible by heterodyne detection (Livet *et al.*, 2006). It is also clear that, owing to these shear-induced effects, the dynamics are not isotropic. The results detailed here show that for a transverse flow geometry (scattering wavevector $\mathbf{q} \perp \mathbf{v}$) the scalar products $\mathbf{q}\cdot\delta\mathbf{v}$ are all zero, and the relaxation times measured in a homodyne XPCS experiment are independent of the flow and measure only the diffusive dynamics of the particles. This result is not generally valid, and, in particular, the dynamics are strongly affected in the longitudinal flow (*i.e.* $\mathbf{q} \parallel \mathbf{v}$) direction. In this situation, the decay profile of the correlation functions are altered by the flow-induced distribution of particle velocities, and it is difficult, or impossible, to 'extract' their diffusive behavior.

2. Description of the experiments

The sample, a suspension of sterically stabilized polymethylmethacrylate (PMMA) particles dispersed in *cis*-decalin, is a well characterized hard-sphere model system (Moussaïd *et al.*, 2008). Here the radius a of the PMMA particles was $\sim$255 nm (with a size polydispersity of 7%) and the colloid volume fraction was $\Phi = 0.16$. The flow cell was made out of a quartz capillary tube with a diameter of $\sim$980 µm (inset in Fig. 1*a*). The (relatively) large diameter of the capillary was chosen to increase the sample volume and the total scattering cross section which is often the limiting factor for XPCS. A syringe pump was pushing the fluid through $\sim$1 mm Teflon tubes into the capillary.

Some important aspects about the fluid behavior, and in particular the laminar character of the flow, are determined by the relative ratio of the inertial to viscous forces. This ratio is expressed as the Reynolds number (Atencia & Beebe, 2005),

$$\mathrm{Re} = vd\rho/\eta. \tag{1}$$

Here d is the characteristic length of the system (in our case the capillary diameter $d = 2R$), ρ is the fluid density, v is the volume flow velocity (measured by the volume flow rate $Q = \pi R^2 v$) of the fluid and η is the dynamic viscosity. The onset of turbulent flow occurs at Reynolds numbers larger than $\sim$1000. In all the experiments reported here, the Reynolds numbers have values that are much smaller ($\mathrm{Re} < 0.1$) which ensures a laminar flow. The main results of this paper, showing the (purely) diffusive nature of the dynamics measured in a transverse flow geometry, confirm this conclusion.

The exact velocity profile in the capillary is determined by the volume flow rate and the details about the boundary conditions at the capillary–fluid interface. In the results reported here, a simplified picture is adopted, and the flow is considered to be characterized by a single (average) shear rate $\dot\gamma = \mathrm{d}v/\mathrm{d}x$. Assuming a no-slip boundary conditions model, the magnitude of this shear rate can be estimated by

$$\dot\gamma = 3v/R. \tag{2}$$

The XPCS experiments were performed in small-angle X-ray scattering geometry (Fig. 1) using partially coherent X-rays at the ID10A beamline (Troïka) of the European Synchrotron Radiation Facility. A single-bounce Si(111) crystal monochromator was used to select 8 keV X-rays, having a relative bandwidth of $\Delta\lambda/\lambda \simeq 10^{-4}$. Higher-order light was suppressed by a Si mirror downstream of the monochromator, and a transversely coherent beam was defined by a pinhole of diameter $s = 10$ µm, placed 0.2 m upstream of the sample. The parasitic scattering from the pinhole was limited by a guard slit (corner) placed in front of the sample. Under these conditions the flux through the pinhole was $\sim 10^9$ photons s^{-1}. The scattering from the PMMA particles was recorded by a 0D scintillator detector (Cyberstar) located 2.3 m downstream of the sample. The detector area was limited to a few speckle size (typically 50–100 µm) by precision slits in front of the detector. Static data were also obtained using a CCD area detector with 22.5 µm pixel size placed at the same distance (Fig. 1).

The intensity autocorrelation functions,

$$g^{(2)}(\mathbf{q}, t) = \frac{\langle I(\mathbf{q}, 0) I(\mathbf{q}, t)\rangle}{\langle I(\mathbf{q}, t)\rangle^2}, \tag{3}$$

were obtained using a digital real-time hardware correlator (from http://www.correlator.com/) connected to the X-ray detector. Assuming a Gaussian distribution of the temporal intensity fluctuations at a fixed $\mathbf{q}$, the intensity correlation functions are related to the dynamic structure factor or intermediate scattering function $f(\mathbf{q}, t)$ *via* the Siegert relationship, $g^{(2)}(\mathbf{q}, t) = 1 + \beta|f(\mathbf{q}, t)|^2$. Here β is the speckle contrast, in this set-up around 5% depending on the exact pinhole and detector slit sizes.

3. XPCS in a laminar flow

The correlation functions measured in an XPCS experiment on a fluid undergoing shear flow are determined by several factors: (i) the (shear enhanced) diffusive motion of the particles; (ii) the shear-induced distribution of average flow velocities, or more precisely the Doppler shifts coming from particles moving with different average velocities in the scattering volume; (iii) the (average) transit time of the particles through the scattering volume. Each of these effects will be discussed in the following.

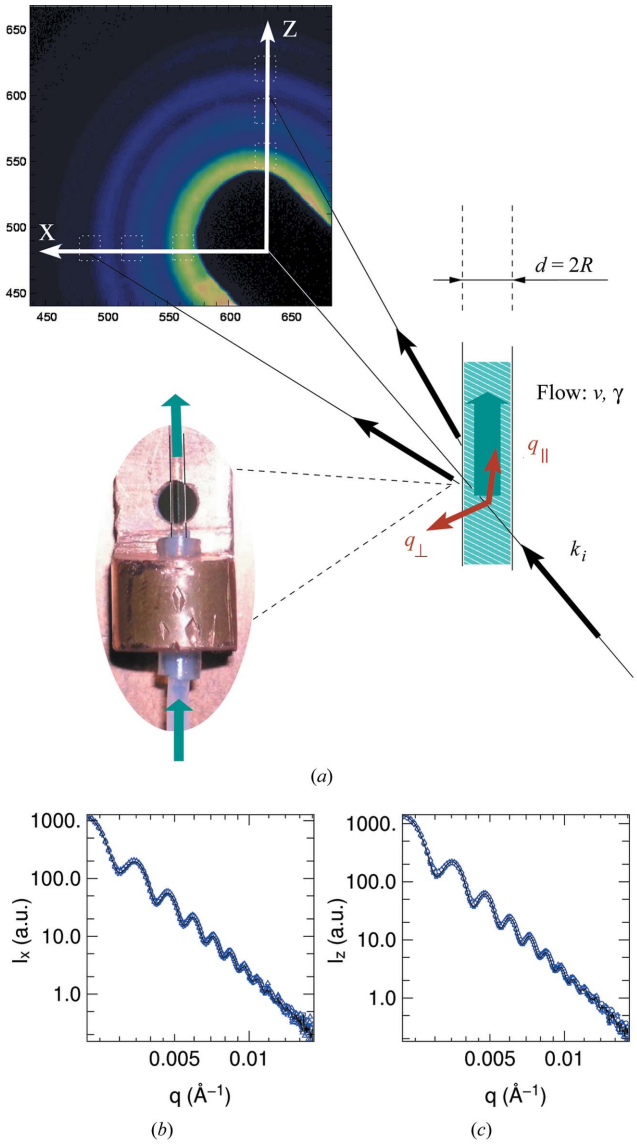

Figure 1
(*a*) Small-angle X-ray experimental set-up and flow chamber for the XPCS experiments. Static scattering, I_x, I_z, for the two flow geometries considered here: transverse, $\mathbf{q} \perp \mathbf{v}$ (*b*) and longitudinal, $\mathbf{q} \parallel \mathbf{v}$ (*c*). The data were recorded at several flow rates (v = 0–200 µm s^{-1}). In the q range accessible here, the static properties are both isotropic and flow-independent.

The diffusive motion of the colloidal particles is enhanced by the shear. This effect has been studied using DLS by Ackerson & Clark (1981). The contribution of thermal diffusion to the intermediate scattering function of a colloidal suspension in a shear flow is shown to be described by

$$f_{\rm D}(\mathbf{q}, t) = \exp\left[-\Gamma t\left(1 - \frac{q_\parallel q_\perp}{q^2}\dot\gamma t + \frac{q_\parallel^2}{q^2}\frac{(\dot\gamma t)^2}{3}\right)\right]. \quad (4)$$

Here $\mathbf{q}$ is the scattering wavevector with Cartesian components $q_\parallel$ and $q_\perp$ (parallel and perpendicular, respectively, to the direction of the flow) and absolute value q, $\dot\gamma$ is the shear rate (considered uniform) and Γ is the relaxation rate which relates to q and the diffusion constant D_0 *via*

$$\Gamma = D_0 q^2.$$

In a transverse flow scattering geometry $q_\parallel = 0$, hence equation (4) is independent of the flow (shear), and becomes indistinguishable from the intermediate scattering function of a suspension undergoing a simple Brownian motion, $f_\perp(q, t) = \exp(-D_0 q^2 t)$.

The relevant time scale associated with thermal diffusion, the diffusion time, can thus be defined as

$$\tau_{\rm D} = \frac{1}{\Gamma} = \frac{1}{D_0 q^2}. \quad (5)$$

As was shown in a number of Doppler velocimetry experiments (Fuller *et al.*, 1980; Narayanan *et al.*, 1997), the intensity correlation functions are not only determined by the diffusive motion of the colloids [equation (4)] but are also modulated by a self-beat frequency created by particles moving with different average (flow) velocities. If the (shear-induced) velocity difference between two particles separated by a distance $\mathbf{r} = \mathbf{r}_1 - \mathbf{r}_2$ is $\delta\mathbf{v}$, the resulting beating frequency is given by $\mathbf{q}\cdot\delta\mathbf{v}(r)$. This shear-induced effect can be detected only in 'non-transverse' scattering geometries when the scalar product $\mathbf{q}\cdot\delta\mathbf{v}$ is different from zero. The resulting intensity correlation function is thus modulated by an average over all the Doppler shifts between all pairs of particles in the scattering volume, which can be written as

$$G_{\delta v}(\mathbf{q}, t) = \frac{1}{R^2}\int_0^R {\rm d}r_1 \int_0^R {\rm d}r_2 \exp[-i\mathbf{q}\cdot\delta\mathbf{v}(r)t]. \quad (6)$$

In the case of a uniform shear, the double integral in equation (6) can be calculated analytically (Narayanan *et al.*, 1997), leading to

$$G(\mathbf{q}, t) = \left[\frac{\sin(\Gamma_{\rm S} t)}{\Gamma_{\rm S} t}\right]^2, \quad (7)$$

where the shear relaxation rate $\Gamma_{\rm S}$ depends on q and the flow velocity v (or equivalently on the flow rate $\dot\gamma$) and is given by $\Gamma_{\rm S} = q_\parallel v$. A characteristic time scale associated with the shear-induced effects, the shear time $\tau_{\rm S}$, can thus be defined as

$$\tau_{\rm S} = \frac{1}{\Gamma_{\rm S}} = \frac{1}{v q_\parallel}. \quad (8)$$

The diffusion-induced [equation (4)] and shear-induced [equation (7)] effects to the intermediate scattering functions were shown to be independent (Fuller *et al.*, 1980); hence the correlation functions measured in an XPCS experiment under laminar flow can be written

$$g^{(2)}(\mathbf{q}, t) - 1 = \beta \exp\left[-2\Gamma t\left(1 - \frac{q_\perp q_\parallel}{q^2}\dot\gamma t + \frac{q_\parallel^2}{q^2}\frac{(\dot\gamma t)^2}{3}\right)\right] \times \left[\frac{\sin(\Gamma_{\rm S} t)}{\Gamma_{\rm S} t}\right]^2. \quad (9)$$

The relative importance of the shear-induced effects compared with thermal diffusion is quantified by the ratio between the diffusion time [equation (5)] and the shear time [equation (8)],

$$S = \frac{\tau_D}{\tau_S} = \frac{v q_\parallel}{D_0 q^2}, \qquad (10)$$

which will be referred to as the shear number.

In order to measure the diffusion time τ_D, the shear number must be kept low ($S \ll 1$). Fortunately, the shear-induced effects are visible only in a non-transverse scattering geometry, and from equation (10) it results that a practical means to measuring the thermal diffusion of the scatterers is to keep the scattering wavevector perpendicular to the flow velocity ($q_\parallel = 0$). For any other scattering geometries, the shear number will be too high for almost all interesting combinations of the experimental parameters ($\dot\gamma$, D_0 *etc.*), and the effect of thermal diffusion will be 'washed out' by the much faster decay of $g^{(2)}$ owing to the shear time.

The continuous flow of particles through the scattering volume introduces a third relevant time scale, the transit time. Its relative importance compared with thermal diffusion is determined by the magnitude of the Deborah number, the ratio between the correlation (diffusion) time τ_D and the transit time,

$$\mathrm{De} = \tau_D v/s. \qquad (11)$$

Here v is the (average) flow velocity and s is the transverse beam size ($s = 10$ µm). The Deborah number is a quantity that depends not only on the flow rate and beam size but also on the q value (through τ_D); however, in all the measurements reported here, De was smaller than 0.1 even at the highest flow rates and smallest values of q. Consequently, in the current analysis, the effects induced by the finite transit time of the particles through the scattering volume were neglected and only the dominant effects related to the Brownian motion and the Doppler-shift-induced decays of the correlation functions were considered.

In conclusion, in the limits of small De numbers ($\mathrm{De} \ll 1$) and for a laminar flow characterized by a single shear constant $\dot\gamma$, we expect the correlation functions measured in an XPCS experiment to be described by equation (9). As will be seen in the following section, the correlation functions measured in a transverse or a longitudinal flow geometry are well fitted by this form (Figs. 2 and 3).

4. Results: dynamics of PMMA colloids in laminar flow

The dynamics of the colloidal suspension of PMMA hard spheres was probed in transverse and longitudinal flow geometries at average flow velocities ranging between 0 and 200 µm s^{-1} and for q values in units of qa (a is the particle radius) ranging between 3 and 10. At these high values of q (on scales comparable with or smaller than the particle size) and for the low shear rates probed here the time-averaged static properties are both isotropic and flow-independent (Figs. 1*b* and 1*c*).

The dynamical properties are, however, not isotropic. The intensity autocorrelation functions [equation (9)] can be written for the scattering geometries probed here, leading to

$$\mathbf{q} \perp \mathbf{v} \qquad g^{(2)}(q,t) = 1 + \beta \exp(-2\Gamma t), \qquad (12)$$

$$\mathbf{q} \parallel \mathbf{v} \qquad g^{(2)}(q,t) = 1 + \beta \exp(-2\Gamma t)\left[\frac{\sin(\Gamma_S t)}{\Gamma_S t}\right]^2. \qquad (13)$$

Here the shear-induced corrections to the diffusive dynamics in equation (9) of the order of $\dot\gamma t$ and $(\dot\gamma t)^2$ were neglected because they are too small to be measured/fitted. Also, the shear relaxation rate Γ_S could be related *via* a rheological model [*e.g.* by using equations (2) and (8)] to a shear rate $\dot\gamma$. This would be important if the goal was to measure the shear rate, but here the focus is on the measurement of the diffusion dynamics (*i.e.* Γ), hence the shear relaxation rates Γ_S were simply obtained from the fits with equation (13) and not related to a shear rate.

It should also be mentioned that the X-ray contrast β was around 4–5% for all the experiments reported here, independent of the scattering geometry and of the flow rate. This agrees quite well with calculated values, and proves that the Deborah numbers were low enough to prevent a significant reduction of β by the flow, and that the size and shape of the coherent beam and of the speckles were symmetric enough to prevent any anisotropy induced by the scattering geometry.

Correlation functions measured for $\mathbf{q} \perp \mathbf{v}$ at three different values of q, and fits with equation (12), are shown in Fig. 2. The correlation functions obtained at zero flow (filled symbols) are shown together with those measured at an average flow velocity of $v \simeq 58.5$ µm s^{-1} (empty symbols). The fits were performed for all the correlation functions, but for clarity only those corresponding to the $v = 58.5$ µm s^{-1} data are shown (solid lines). As can be seen, the correlation functions with and without flow are almost identical, showing that at these shear rates they are basically unaffected by the flow.

This conclusion is not valid for non-transverse flow geometries. Examples of correlation functions measured in longitudinal flow ($\mathbf{q} \parallel \mathbf{v}$) are shown in Fig. 3. Here, functions measured at a single wavevector q with a static sample ($v = 0$ µm s^{-1}, panel *a*) are shown together with the correlations measured at two different flow rates, corresponding to average flow velocities of $v = 11.7$ µm s^{-1} (*b*) and $v = 23.4$ µm s^{-1} (*c*). In the absence of flow, the correlation functions are still well described by simple exponential decays (Fig. 3*a*) allowing the diffusion relaxation rates Γ to be obtained. These values are, within experimental errors, comparable with those obtained from $\mathbf{q} \perp \mathbf{v}$ [see zero flow data (squares and circles) in Fig. 4]. The measured diffusion coefficient is $D \simeq 1.7 \times 10^7$ Å^2 s^{-1}, with an estimated uncertainty of ∼15%.

The relaxations obtained from a flowing sample in longitudinal flow geometry (Figs. 3*b* and 3*c*) are strongly affected by the flow. Even though the flow velocities are smaller than those shown in Fig. 2 for $\mathbf{q} \perp \mathbf{v}$, the effects on the correlation times and on the shape of the correlation functions are important. The solid lines show the fits to the experimental data with equation (13). In principle, both relaxation rates, Γ and Γ_S, could be obtained from a single fitting procedure, but owing to the strong influence of the shear-induced effects (high shear number) this is unfortunately not the case. Even at

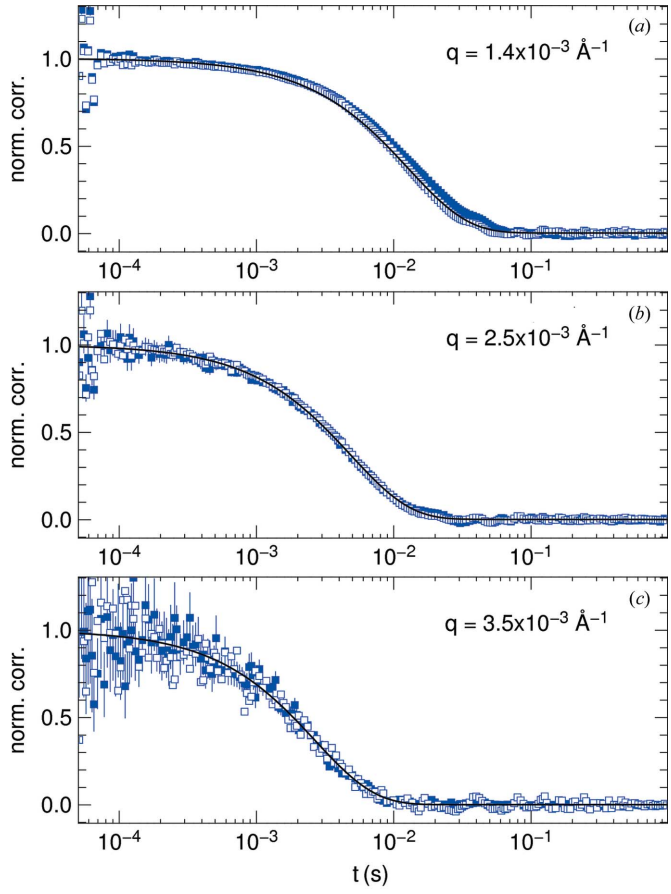

Figure 2
Normalized correlation functions $[g^{(2)}(\mathbf{q}, t) - 1]/\beta$ obtained in a transverse flow geometry ($\mathbf{q} \perp \mathbf{v}$), shown here for three different values of q at zero flow (filled symbols) and at $v \simeq 58.5$ µm s^{-1} (empty symbols). It can be seen that for this flow rate the influence of the shear flow on the correlation function is, in the first order, negligible. The solid lines show fits to the $v \simeq 58.5$ µm s^{-1} data with equation (12).

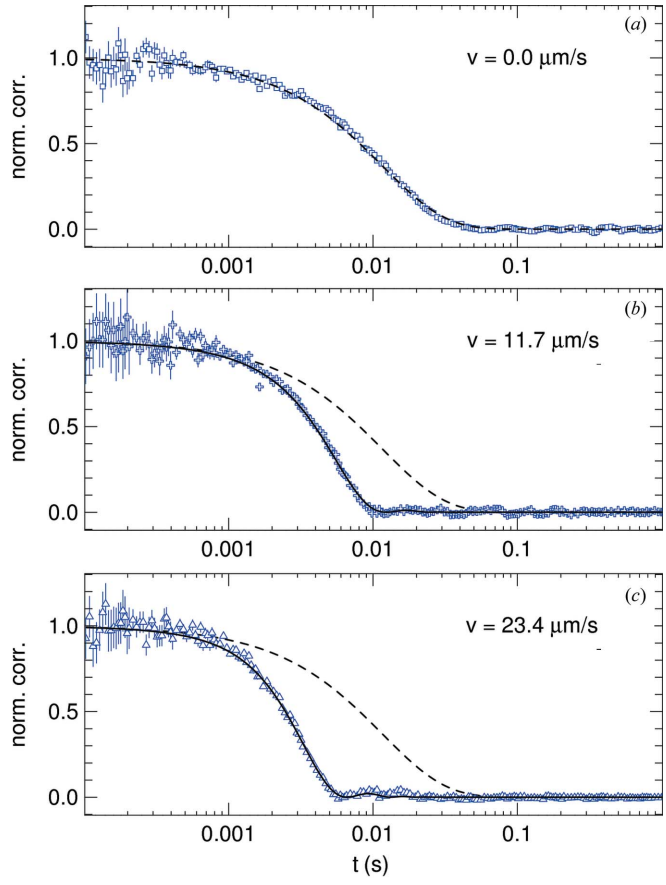

Figure 3
Normalized correlation functions $[g^{(2)}(\mathbf{q}, t) - 1]/\beta$ obtained in longitudinal flow scans ($\mathbf{q} \parallel \mathbf{v}$), at $q = 1.3 \times 10^{-3}$ Å^{-1} and three different flow velocities: $v = 0$ (*a*), 11.7 (*b*) and 23.4 µm s^{-1} (*c*). The solid lines are least-square fits with equation (13). The dashed lines show the fits to the zero-flow correlation function (panel *a*).

very small flow velocities (*e.g.* those used in Figs. 3*b* and 3*c*), the estimated shear numbers for a longitudinal scattering wavevector $q_{\parallel} = 1.3 \times 10^{-3}$ Å^{-1} are $S \simeq 3.6$ (*b*) and $S \simeq 7.2$ (*c*). As a consequence, the intensity correlation functions are dominated by the shear time if a non-transversal flow geometry is used, and the errors on the fitted values for Γ are high.

It should also be mentioned that the oscillations which can be noticed on some of the correlation functions at long times (Figs. 2 and 3) are not due to the shear effects described by equation (13). As they tend to appear/disappear on a more 'random' basis, a possible explanation would be that bubbles or other impurities sometimes sweep through the scattering volume. As the statistical error bars are smaller at longer times, such artifacts may appear like real effects.

In order to measure the diffusive dynamics of the particles under flow, the correlation times (relaxation rates) must be obtained from the $\mathbf{q} \perp \mathbf{v}$ data. The dispersion relationships for the diffusion coefficient $D = \Gamma q^{-2}$ measured in transverse flow scans at zero flow as well as two (relatively) high-flow velocities $v = 58.5$ µm s^{-1} and $v = 117$ µm s^{-1} are shown in Fig. 4. As expected for a suspension undergoing Brownian motion,

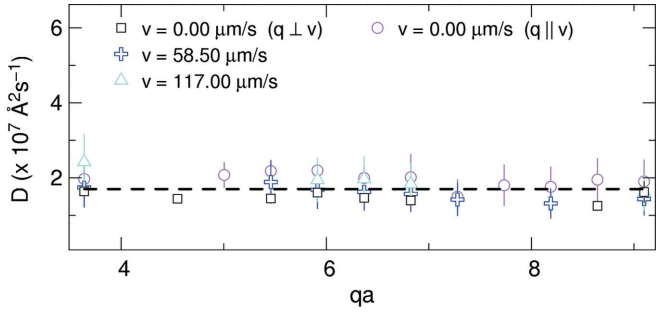

Figure 4
Diffusion constant D associated with the dynamics of the colloidal particles (radius a) in shear flow as a function of q measured in a transverse flow ($\mathbf{q} \perp \mathbf{v}$) geometry for three volume flow rates (squares, crosses and triangles). Values for the diffusion coefficient obtained from longitudinal flow scans ($\mathbf{q} \parallel \mathbf{v}$) with static samples are also shown (circles). The dashed line shows the estimated value for the diffusion constant (see text).

the correlation times measured at $v = 0$ and $v = 58.5$ µm s^{-1} decay as q^{-2} and the diffusion coefficient is q-independent. In addition, one can observe that in this scattering geometry the measured relaxation rates (and the diffusion coefficient) are also flow-independent. This conclusion holds to a certain

degree for the $v = 117$ μm s^{-1} data as well, although at lowest values of q the measured diffusion coefficients start being enhanced by the shear.

The diffusion coefficient can also be estimated using the Einstein–Stokes relationship,

$$D_0 = k_B T/6\pi\eta a. \quad (14)$$

The viscosity of the solvent is $\eta_0 \simeq 3.0 \times 10^{-3}$ Pa s, and the viscosity of the solution is approximately (Segrè *et al.*, 1995) $\eta \simeq 1.5\eta_0 = 4.5 \times 10^{-3}$ Pa s. With values corresponding to our experimental conditions ($T \simeq 295$ K and $a \simeq 255$ nm), the resulting diffusion coefficient is $D_0 \simeq 1.88 \times 10^7$ Å^2 s^{-1}, which is in good agreement with the values measured by XPCS ($D \simeq 1.7 \times 10^7$ Å^2 s^{-1}, dashed line in Fig. 4). The small discrepancy could be attributed to a slightly different viscosity of the solution and/or to small hydrodynamic effects.

5. Conclusions

The method presented here allows the direct measurement of mesoscale dynamics in a complex fluid under laminar flow, and can be used to obtain diffusion coefficients and/or to retrieve information about particle size, rheological properties of the solvent *etc.* in a variety of X-ray-sensitive samples.

The flow-induced transit-time effects are negligible for most of the interesting combinations of sample and flow properties except perhaps the most viscous suspensions (Busch *et al.*, 2008), but the measured correlation functions are, in most situations, strongly affected by the shear time. The basic idea of the method presented here is to keep the shear-induced effects on the correlation functions as low as possible by choosing a transverse flow geometry ($\mathbf{q} \perp \mathbf{v}$) and a low-enough shear rate.

For a perfect transverse flow alignment, $q_\parallel = 0$ and the shear time [equation (8)] is infinity. As a consequence, the shear number is zero and an XPCS experiment measures only the diffusion time. In practice, such a perfect alignment does not exist and a more realistic shear number [equation (10)] can be written as

$$S = v\varphi/D_0 q, \quad (15)$$

where φ is a small misalignment angle (in radians) of the flow channel with respect to the longitudinal direction.

Setting an upper limit on the shear number (*e.g.* $S \simeq 0.1$) in order to keep the shear-induced effect low leads to a maximum acceptable value for the shear rate $\dot\gamma$ (Salmon *et al.*, 2008). This value is dependent on the exact nature of the sample (D_0), on the scattering wavevector q and on the particular alignment (angle φ).

The experimental conditions under which it is possible to measure the diffusive dynamics of the particles can be 'visualized' in Fig. 5. Here the dispersion relationships for the diffusion rate Γ and the shear relaxation rate $\Gamma_S = v\varphi q$ (assuming a 'nearly transverse' flow geometry with a small misalignment angle φ) were plotted together with the (q-independent) transit rate. As stated above, the shear and Deborah numbers must be much smaller than unity, or equivalently the diffusion relaxation rate must be much higher than the shear- and transit-induced relaxation rates. With the values chosen as an example in Fig. 5, $\varphi = 0.01$ (corresponding to an assumed misalignment of $\sim 0.6^\circ$), $D = 1.7 \times 10^7$ Å^2 s^{-1} and a flow velocity of $v = 58.5$ μm s^{-1}, this condition is fulfilled for the q range accessible by XPCS (highlighted by the thick solid line), and the relaxation rates measured at $v = 0$ and 58.5 μm s^{-1} confirm that these conditions are fulfilled. At the same time it is clear that this would not be the case if the flow velocity increased beyond a maximum acceptable value, or if the measurements were performed at smaller q, for instance by DLS. The maximum flow velocity that allows measurements of the diffusive dynamics depends on the sample (time scales that have to be measured), the flow geometry and the scattering alignment. The study presented here is a proof of principle, and the data show that the transverse flow alignment was achieved with an accuracy better than $\sim 0.5^\circ$, and that flow velocities up to $\sim$50–100 μm s^{-1} allow measurements of the diffusive dynamics of the colloidal suspension. In principle, such a value (*e.g.* for the maximum acceptable flow velocity) could be used as a reference, and it should be possible to scale it in order to determine the experimental conditions that allow measurements of the diffusive dynamics on different samples with different relaxation times. These ideas will be explored in further studies.

The method described here also allows measurements of various properties of the laminar flow (*e.g.* using the shear relaxation rates Γ_S measured in a longitudinal flow geometry to calculate the shear rate $\dot\gamma$). While this is a valid aim (Fuller *et al.*, 1980; Narayanan *et al.*, 1997), it was not our purpose here. We intended to demonstrate that the diffusive dynamics are accessible in a flowing sample. We believe that measuring

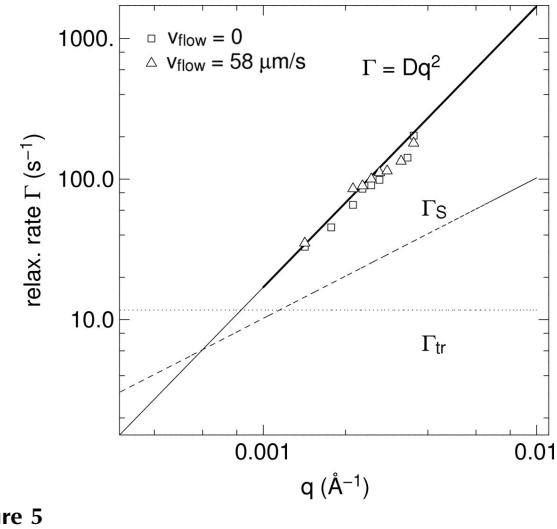

Figure 5
Dispersion relationships for the diffusion ($\Gamma = Dq^2$), shear ($\Gamma_S = v\varphi q$) and transit ($\Gamma_{tr} = v/s$) relaxation rates. The (example) values used here to estimate Γ, Γ_S and Γ_{tr} were $D = 1.7 \times 10^7$ Å^2 s^{-1}, $\varphi = 0.01$ (0.5°) and $v = 58.5$ μm s^{-1}. The thick solid line highlights the q region that could, in principle, be accessed by XPCS. With the flow parameters chosen here, this is also the region where the thermal diffusion dominates the dynamic signal and can be measured by XPCS. The experimental points show the relaxation rates measured with the static, $v = 0$ (squares), and the $v = 58.5$ μm s^{-1} (triangles) samples.

the 'intrinsic' dynamical properties of the fluid sample in a microfluidic experiment/set-up provides a tremendous amount of interesting opportunities for XPCS experiments in soft-matter and biological systems. The minimal requirements for such experiments would be a strong enough scattering from the sample, *e.g.* $\sim$1 photon per speckle per correlation time if a two-dimensional area detector is used, and a flow/shear rate which is fast enough to prevent beam damage but small enough to allow the measurement of diffusive dynamics in the presence of shear.

We wish to acknowledge helpful discussions with Narayanan Theyencheri, Jean-Baptiste Salmon, Fanny Destremaut, Yuriy Chushkin, Sebastian Busch, Erik Geissler and Mark Sutton.

References

Ackerson, B. J. & Clark, N. A. (1981). *J. Phys. (Paris)*, **42**, 929–936.
Atencia, J. & Beebe, D. J. (2005). *Nature (London)*, **437**, 648–655.
Banchio, A. J., Gapinski, J., Patkowski, A., Haüssler, W., Fluerasu, A., Sacanna, S., Holmqvist, P., Meier, G., Lettinga, M. P. & Nägele, G. (2006). *Phys. Rev. Lett.* **96**, 138303.
Berne, B. & Pecora, R. (2000). *Dynamic Light Scattering.* New York: Dover.
Bilderback, D. H., Elleaume, P. & Weckert, E. (2005). *J. Phys. B*, **38**, S773–S797.
Busch, S., Jensen, T., Chushkin, Y. & Fluerasu, A. (2008). *Eur. Phys. J. E.* Accepted.
Falus, P., Borthwick, M. A., Narayanan, S., Sandy, A. R. & Mochrie, S. G. J. (2006). *Phys. Rev. Lett.* **97**, 066102.
Fluerasu, A., Moussaïd, A., Madsen, A. & Schoffield, A. (2007). *Phys. Rev. E*, **76**, 010401(R).
Fuller, G. G., Rallison, J. M., Schmidt, R. L. & Leal, L. G. (1980). *J. Fluid Mech.* **100**, 555–575.
Livet, F., Bley, F., Ehrburger-Dolle, F., Morfin, I., Geissler, E. & Sutton, M. (2006). *J. Synchrotron Rad.* **13**, 453–458.
Moussaïd, A. *et al.* (2008). In preparation.
Narayanan, T., Cheung, C., Tong, P., Goldburg, W. & Wu, X.-L. (1997). *Appl. Opt.* **36**, 7639.
Pollack, L., Tate, M. W., Finnefrock, A. C., Kalidas, C., Trotter, S., Darnton, N. C., Lurio, L., Austin, R. H., Batt, C. A., Gruner, S. M. & Mochrie, S. G. J. (2001). *Phys. Rev. Lett.* **86**, 4962–4965.
Salmon, J.-B. *et al.* (2008). In preparation.
Segrè, P. N., Meeker, S. P., Pusey, P. N. & Poon, W. C. K. (1995). *Phys. Rev. Lett.* **75**, 958–961.
Shenoy, G. K. (2003). *Nucl. Instrum. Methods*, A**199**, 1–9.
Sutton, M. (2002). In *Third-Generation Hard X-ray Synchrotron Radiation Sources: Source Properties, Optics, and Experimental Techniques*, edited by Dennis M. Mills. New York: John Wiley.
Sutton, M., Mochrie, S. G. J., Greytak, T., Nagler, S. E., Berman, L. E., Held, G. A. & Stephenson, G. B. (1991). *Nature (London)*, **352**, 608–610.